β-Fused Oligoporphyrins: A Novel Approach to a New Type of Extended Aromatic System

Roberto Paolesse,*,† Laurent Jaquinod,‡ Fabio Della Sala,§ Daniel J. Nurco,‡ Luca Prodi,⊥ Marco Montalti,⊥ Corrado Di Natale,§ Arnaldo D'Amico,§ Aldo Di Carlo,§ Paolo Lugli,§ and Kevin M. Smith*,‡

Contribution from the Dipartimento di Scienze e Tecnologie Chimiche, Università di Roma "Tor Vergata", Via della Ricerca Scientifica, 00173 Roma, Italy; Department of Chemistry, University of California, Davis, California 95616; Dipartimento di Ingegneria Elettronica and INFM, Università di Roma "Tor Vergata", Via di Tor Vergata 110, 00173 Roma, Italy; and Dipartimento di Chimica "G. Ciamician", Università di Bologna, Bologna, Italy

Received April 14, 2000

Abstract: A novel trimeric porphyrin array in which the macrocycles are directly fused through their β-pyrrolic carbons has been prepared and investigated. These molecules feature a 7,8,17,18-tetraethylporphyrin moiety flanked on opposite sides by two tetraphenylporphyrin (TPP) moieties. The 2,3 and 12,13 β-carbon positions of the tetraethylporphyrin substructure also function as the β-carbons in the 2 and 3 positions of the two TPP macrocycles. This framework was prepared via the reaction of 2,5-bis[(*N*,*N*,*N*-trimethylammonium)methyl]-3,4-diethylpyrrole diiodide with the nickel(II) complex of pyrrolo[3,4-*b*]-5,10,15,20-tetraphenylporphyrin, which afforded a 62-π-electron 72-atom macrocycle (**2**) with a central free-base tetraethylporphyrin and two terminal nickel(II) TPP functionalities. The tri-free-base complex (**1**) was obtained by treatment of the dinickel(II) complex with sulfuric acid followed by neutralization. Crystallographic characterization of **1** (as its tetracation salt) and **2** (as its dication salt) revealed that this type of molecule bears a considerable degree of macrocyclic flexibility. Luminescence spectra of **1** displayed an intense band around 800 nm, making these types of macrocycles promising candidates as chromophores for labels and sensors in biological media. Both **1** and **2** exhibited complex optical spectra, each of which displayed an intensely red shifted Q-band [**1**, λ_{max} (nm) 369 (ϵ 36 400), 416 (49 700), 488 (71 200), 562 (16 500), 650 (15 700), 744 (42 300); **2**, λ_{max} nm 361 (ϵ 87 200), 408 (107 000), 486 (189 000), 558 (27 700), 650 (28 200), 682 (31 100), 716 (175 500)]. Selective protonation of **1** with TFA afforded a green tetracationic species [$(H_4-H_2-H_4)^{4+}$·**1**] with an even more red-shifted Q-band (848 nm) while addition of excess TFA yielded a red hexaprotonated species [$(H_4-H_4-H_4)^{6+}$·**1**]. Optical analyses of **1**, using the INDO/SCI and orbital localization techniques, were performed to obtain information with regard to the degree of macrocyclic π-electron delocalization. These studies showed that the optical properties of **1** cannot be described within the excitonic model of weakly interacting macrocycles ($\alpha > 60\%$), and that π-electron delocalization over the 72-atom macrocycle is not complete. Even though resonance structures for the 72-atom macrocycle imply a fully conjugated aromatic system, our data indicated that the three constituent porphyrin macrocycles behave somewhat more like discrete aromatic systems.

Introduction

The design and preparation of oligomeric nanoarchitectures able to communicate over large distances has been an important area of research in the past few years.[1] Successful synthetic approaches to these molecules, which might serve as molecular devices, will have an enormous impact on many fields. Nanoelectronic applications, for example, provide substantial incentives to conduct research relating to molecular information processing and storage devices, molecular wires, and nanosensory devices. The capability of oligoporphyrinic frameworks to serve as useful electrochemical devices is well documented. Nature gives us an admirable example of such a process in photosynthetic systems by organizing a 3-dimensional array of several porphyrins which enable the energy- and electron-transfer processes necessary for the conversion of sunlight energy into ATP.[2] In these complex arrays, properties of individual chromophores are fine-tuned by the scaffolding provided by the photosynthetic reaction center (PRC) protein. One such function of the PRC protein is to hold the porphyrinic chromophores in groupings of two or more (i.e., the "special pair") to facilitate the photosynthetic process. Oligoporphyrin arrays, which have aptly demonstrated their utility in natural

* To whom correspondence should be addressed. Phone: (530) 752-4091. Fax: (530) 754-2100. E-mail: kmsmith@ucdavis.edu.

† Dipartimento di Scienze e Tecnologie Chimiche, Università di Roma "Tor Vergata".

‡ University of California.

§ Dipartimento di Ingegneria Elettronica and INFM, Università di Roma "Tor Vergata".

⊥ Università di Bologna.

(1) (a) *Handbook of Organic and Conductive Molecules and Polymers*; Nalwa, S. H., Ed.; Wiley: Chichester, U.K., 1997. (b) Tour, M. J. *Chem. Rev.* **1996**, *96*, 537.

(2) (a) Deisenhofer, J.; Epp, O.; Miki, K.; Huber, R.; Michel, H. *J. Mol. Biol.* **1984**, *180*, 385. (b) Deisenhofer, J.; Epp, O.; Miki, K.; Huber, R.; Michel, H. *Nature* **1985**, *318*, 618. (c) Deisenhofer, J.; Michel, H. *Science* **1989**, *245*, 1463. (d) Kühlbrandt, W.; Da Neng, W.; Fujiyoshi, Y. *Nature* **1994**, *367*, 614. (e) McDermott, G.; Prince, S. M.; Freer, A. A.; Hawthornthwaite-Lawless, A. M.; Papiz, M. Z.; Cogdell, R. J.; Isaacs, N. W. *Nature* **1995**, *374*, 517.

10.1021/ja001316+ CCC: $19.00
Published on Web 11/02/2000

systems, now pose a formidable task to synthetic chemists with the aim of producing functional molecular scale devices.

Covalently linked porphyrin oligomers are potential precursors for building such electron- and energy-transfer devices, and many such molecules have been reported. Geometry, distance, and relative orientation between each chromophore, the nature of the bridges between porphyrin components, the extent of steric interactions (if any), and the connectivity of the porphyrins are to be considered for the design and development of a functional porphyrin array. Alkyne-bridged oligoporphyrinic systems, obtained from the Pd-catalyzed reactions of a small set of alkynyl- and bromoporphyrin building blocks, have been of particular interest. These materials display significant changes in their optical and electrochemical properties particularly when the alkynyl groups are attached at the *meso*-positions.[4] The bridging groups enhance the direct conjugation between the essentially coplanar chromophores, resulting in split Soret absorption bands and intensely red shifted Q-bands. Different synthetic approaches have been developed to obtain these oligoporphyrins, and it has also been possible to introduce metal complexes within these *meso*-bridging groups.[5]

While many covalently linked oligoporphyrin arrays have been reported, there are, however, only a few in which the coplanarity and π-overlap of their individual porphyrin rings are enforced by rigid fused aromatic bridges. Such arrays should display a pronounced electronic interaction between metal centers, via the overlap of their d(π)-orbitals, with the conjugated π-system of the coplanar porphyrins. A first approach was explored by Crossley and co-workers, who prepared edge-fused oligomers by condensation of free-base or metalated dione or tetraone porphyrins with aromatic *o*-diamines or 1,2,4,5-tetraamines.[6a,b] Bent or linear polyporphyrins such as **3** ($n = 2$) were prepared to investigate their potential as "molecular wires" and spanned as much as 56 Å.[6c,7] Other fused-porphyrin arrays sharing a common benzene ring have also been prepared.[8] However, the presence of aromatic spacers prevents these edge-fused oligoporphyrins from reaching a fully delocalized conjugation pathway, and these compounds can be considered as arrays of weakly interacting tetrapyrroles.

It remains a challenge to design organic molecules displaying truly long-range π-delocalization. The absence of a spacer and consequently the direct link between porphyrins could dramatically increase the π-electron delocalization over the molecule and yield improved performance in molecular electronic applications. Recently, a straightforward synthesis of [*n*]porphyracene containing doubly *meso*-β -linkages has been reported independently by two Japanese groups.[9,10] Oxidation of nickel(II) or palladium(II) 5,10,15-triarylporphyrins with 1 equiv of hexachloroantimonate gave the dimeric species **4**, whose visible spectra are broader and shifted to longer wavelength compared with those of the corresponding monomers. An intense Q-band was observed in the 734−756 nm region of the optical spectrum. The recent availability of fused pyrroloporphyrins[11] **5**−**8** led us to design and synthesize new π-extended molecules in which two or three porphyrin moieties are directly fused at their β-pyrrolic positions.[12] Herein we describe a new 62-π-electron 72-atom aromatic macrocycle which is a component of our β-fused porphyrin trimers **1** and **2**. Optical properties of **1** have

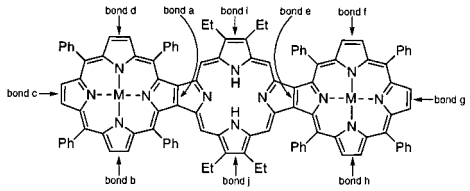

$[Ni\text{-}H_4\text{-}Ni]^{2+} \bullet 2(Cl^-)$ **2**: M = Ni
$[H_4\text{-}H_2\text{-}H_4]^{4+} \bullet 4(CF_3COO^-)$ **1**: M = 4H

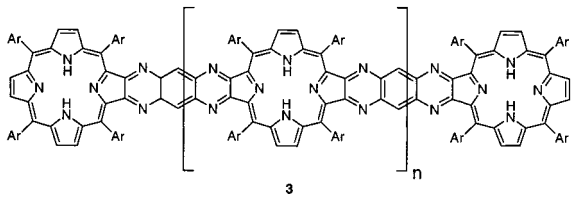

3

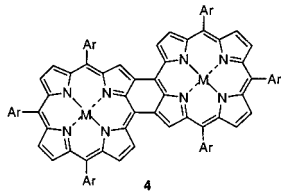

4

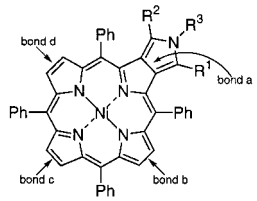

	R^1	R^2	R^3
5	O-tBu	O-Me	H
6	O-iPr	H	H
7	H	H	Me
8	H	H	H

(3) (a) Gust, D.; Moore, T. A. In *The Porphyrin Handbook*; Kadish, K. M., Smith, K. M., Guilard, R., Eds.; Academic Press: Boston, MA, 2000; Vol. 8, p 153. (b) Wasielewski, M. R. *Chem. Rev.* **1992**, *92*, 435. (c) Kurreck, H.; Huber, M. *Angew. Chem., Int. Ed. Engl.* **1995**, *34*, 849.

(4) (a) Lin, V. S.-Y.; DiMagno, S. G.; Therien, M. J. *Science* **1994**, *264*, 1105. (b) Anderson, H. L.; Martin, S. J.; Bradley, D. D. C. *Angew. Chem., Int. Ed. Engl.* **1994**, *33*, 655. (c) Tamiaki, H.; Miyatake, T.; Tanikaga, R.; Holzwarth, A. R.; Schaffner, K. *Angew. Chem., Int. Ed. Engl.* **1996**, *35*, 772. (d) Hsiao, J. S.; Krueger, B. P.; Wagner, R. W.; Johnson, T. E.; Delaney, J. K.; Mauzerall, D. C.; Fleming, G. R.; Lindsey, J. S.; Bocian, D. F.; Donohoe, R. J. *J. Am. Chem. Soc.* **1996**, *118*, 11181 and references therein.

(5) Ferri, A.; Polzonetti, G.; Licoccia, S.; Paolesse, R.; Favretto, D.; Traldi, P.; Russo, M. V. *J. Chem. Soc., Dalton Trans.* **1998**, 4063.

(6) (a) Crossley, M. J.; Burn, P. L. *J. Chem. Soc., Chem. Commun.* **1991**, 1569. (b) Crossley, M. J.; Govenlock, L. J.; Praskai, J. K. *J. Chem. Soc., Chem. Commun.* **1995**, 2379. (c) Reimers, J. R.; Lü, T. X.; Crossley, M. J.; Hush, N. S. *Chem. Phys. Lett.* **1996**, *256*, 353.

(7) (a) Reimers, J. R.; Hall, L. E.; Crossley, M. J.; Hush, N. S. *J. Phys. Chem. A* **1999**, *103*, 4385. (b) Lu, T. X.; Reimers, J. R.; Crossley, M. J.; Hush, N. S. *J. Phys. Chem.* **1994**, *98*, 11878.

(8) (a) Kobayashi, N.; Numao, M.; Kondo, R.; Nakajima, S.-I.; Osa, T. *Inorg. Chem.* **1991**, *30*, 2241. (b) Ishii, K.; Kobayashi, N.; Higashi, K.; Osa, T.; Lelièvre, D.; Simon, J.; Yamauchi, S. *Chem. Commun.* **1999**, 969. (c) Vicente, M. G. H.; Cancilla, M. T.; Lebrilla, C. B.; Smith, K. M. *Chem. Commun.* **1998**, 2355.

(9) Sugiura, K.; Matsumoto, T.; Ohkouchi, S.; Naitoh, Y.; Kawai, T.; Takai, Y.; Ushiroda, K.; Sakata, Y. *Chem. Commun.* **1999**, 1957.

(10) Tsuda, A.; Nakano, A.; Furuta, H.; Yamochi, H.; Osuka, A. *Angew. Chem., Int. Ed.* **2000**, *39*, 558.

(11) (a) Jaquinod, L.; Gros, C.; Olmstead, M. M.; Antolovich, M.; Smith, K. M. *Chem. Commun.* **1996**, 1475. (b) Gros, C. P.; Jaquinod, L.; Khoury, R. G.; Olmstead, M. M.; Smith, K. M. *J. Porphyrins Phthalocyanines* **1997**, *1*, 201.

(12) Jaquinod, L.; Siri, O.; Khoury, R. G.; Smith, K. M. *Chem. Commun.* **1998**, 1261.

been investigated by use of the INDO/SCI technique to provide an estimate of the degree of π-electron delocalization by evaluation of the exciton delocalization over the molecular skeleton.

Experimental Section

^{1}H NMR spectra were obtained in $CDCl_3$ at 300 MHz using a General Electric QE300 spectrometer; chemical shifts are expressed in parts per million relative to chloroform (7.26 ppm). Electronic absorption spectra were measured in CH_2Cl_2 solution using a Hewlett-Packard 8450A spectrophotometer (Davis) and a Perkin-Elmer lambda 16 spectrophotometer (Bologna). Uncorrected emission and corrected excitation spectra were obtained with a Perkin-Elmer LS50 spectrofluorimeter. The fluorescence lifetimes (uncertainty ±5%) were obtained with an Edinburgh single-photon counting apparatus, in which the flash lamp was filled with N_2. Emission spectra in a rigid, transparent methylcyclohexane matrix at 77 K were recorded using quartz tubes immersed in a quartz Dewar filled with liquid N_2. Fluorescence quantum yields were determined using H_2TPP ($\Phi = 0.11$) in deaerated toluene[13] as a reference. To allow comparison of emission intensities, corrections for the different absorbances[14] and phototube sensitivities were performed. A correction for a difference in the refraction index was introduced when necessary.

Crystal Structure Data for 1. Crystals were grown by slow diffusion of MeOH into a $CHCl_3$ solution of $(H_4{-}H_2{-}H_4)^{4+}$•**1** $[C_{112}H_{86}N_{12}{}^{4+}\cdot 4(CF_3COO^-)\cdot 2(CH_3OH)]$. The selected crystal (0.35 × 0.50 × 0.55 mm) had a triclinic unit cell, space group $P\bar{1}$ and cell dimensions $a = 11.932(2)$ Å, $b = 14.041(2)$ Å, $c = 17.250(3)$ Å, $\alpha = 109.831(11)°$, $\beta = 96.220(11)°$, $\gamma = 102.619(11)°$, $V = 2599.8(7)$ Å^3, and $Z = 1$ (FW = 2116.16). Data were collected on a Siemens P4 diffractometer with a rotating anode source [λ(Cu Kα) = 1.54178 Å] at 130(2) K in $\theta/2\theta$ scan mode to $2\theta_{max} = 112.5°$. Of 6833 reflections measured ($+h,\pm k,\pm l$) all were independent and 4624 had $I > 2\sigma$ ($T_{min} = 0.65$, $T_{max} = 0.76$, $\rho_{calcd} = 1.35$ g cm^{-3}, $\mu = 0.851$ mm^{-1}). The structure was solved by direct methods and refined (on the basis of F^2 using all data) by full-matrix least-squares methods with 725 parameters (Siemens SHELXS-97, SHELXL-97). All non-hydrogen atoms were refined with anisotropic thermal parameters. A description of the hydrogen treatment is given in the Supporting Information. An empirical absorption correction was applied.[15] Final R factors were R1 = 0.081 (observed data) and wR2 = 0.236 (all data).

Bis[nickel(II) 5,10,15,20-tetraphenylporphyrinato[2,3-*b*,*l*]]-7,8,17,18-tetraethylporphyrin [(Ni−H_2−Ni)•2]. 2,5-Bis[(*N*,*N*,*N*-trimethylammonium)methyl]-3,4-diethylpyrrole diiodide (**9**) (45 mg, 1.15 equiv) [freshly prepared by quaternization of 2,5-bis(*N*,*N*-dimethylaminomethyl)-3,4-diethylpyrrole[16] with excess methyl iodide in benzene] and nickel(II) pyrrolo[3,4-*b*]-5,10,15,20-tetraphenylporphyrin[11] (**8**) (53 mg, 0.075 mmol) were placed in methanol (10 mL) and tetrahydrofuran (10 mL) in the presence of $K_3Fe(CN)_6$ (300 mg, 0.92 mmol) and refluxed for 1 h under an inert atmosphere. Monitoring by TLC (SiO_2, CH_2Cl_2/cyclohexane, 3/2) showed complete disappearance of **8** and appearance of a less polar compound. The reaction mixture was diluted with CH_2Cl_2 (150 mL) and washed successively with H_2O, 1 M HCl, and finally aqueous $NaHCO_3$. In some instances, oxidation of the intermediate fused porphyrinogen to the fused trimer **2** was incomplete (as shown by TLC) but could be promoted by stirring the CH_2Cl_2 phase overnight with Al_2O_3 (Brockmann Grade I) in the presence of air. The solvent was evaporated, and the residue was purified by chromatography on a silica gel column (silica gel 60, 70−230 mesh) eluting with CH_2Cl_2/cyclohexane, 2/1. Recrystallization from CH_2Cl_2/methanol containing 0.5% NaOH afforded the title compound as a brown solid (11 mg, 18%): mp > 300 °C; UV−vis λ_{max} (nm) 361 (ϵ 87 200), 408 (107 000), 486 (189 000), 558 (27 700), 650 (28 200), 682 (31 100), 716 (175 500); ^{1}H NMR −2.55 (s, 2 H), 1.58 (t, 12 H), 3.55 (q, 8 H), 7.50 (m, 8 H), 7.69 (m, 16 H), 8.04 (m, 8 H), 8.20 (m, 8 H), 8.31 (d, 4 H, β-pyr), 8.55 (d, 4 H, β-pyr), 8.68 (s, 4 H, β-pyr), 8.84 (s, 4 H); Maldi-TOF 1710.4 (MH^+, 100).

Bis(5,10,15,20-tetraphenylporphyrinato-[2,3-*b*,*l*])-7,8,17,18-tetraethylporphyrin [($H_2{-}H_2{-}H_2$)•1]. Trimer (Ni−H_2−Ni)•**2** (15 mg) was stirred in H_2SO_4 (2 mL) for 10 min. The red reaction mixture was poured into water, neutralized with aqueous saturated Na_2CO_3, and extracted twice with CH_2Cl_2. The organic phases were combined, washed with H_2O, and stripped of solvent. The residue was purified by chromatography on a short alumina column (Brockmann grade III) eluting with CH_2Cl_2/cyclohexane, 1/1. The more polar brown band was collected. Recrystallization from CH_2Cl_2/methanol containing 0.5% NaOH afforded the title compound as a brown solid (10 mg, 68%): mp > 300 °C; UV−vis (see Figure 7) λ_{max} (nm) 369 (ϵ 36 400), 416 (49 700), 488 (71 200), 562 (16 500), 650 (15 700), 744 (42 300); ^{1}H NMR −2.66 (s, 2H, NH), −1.53 (s, 4H, NH), 1.53 (t, 12 H), 3.8 (br q, 8 H), 7.86 (m, 24 H), 8.32 (m, 8 H), 8.74 (m, 8 H), 8.90 (br, 4 H), 9.0 (br, 8 H), 9.30 (s, 4 H); Maldi-TOF 1597.8 (MH^+, 100).

Results and Discussion

Synthesis and Characterizations. Under nonacidic conditions, the Mannich pyrrole **9** reacted in refluxing methanol/THF with pyrrolo[3,4-*b*]porphyrin **8** in the presence of $K_3Fe(CN)_6$ to afford the porphyrin trimer (Ni−H_2−Ni)•**2**.[12]

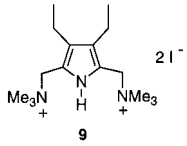

9

Demetalation of **2** with sulfuric acid gave the fused trimer ($H_2{-}H_2{-}H_2$)•**1**. The inner NH protons resonate at −2.66 and −1.56 ppm, integrating for two and four protons, respectively. To a first approximation these chemical shifts, when compared with those of the closely related porphyrins TPP and OEP [(H_2TPP, NH −2.79 ppm) (H_2OEP, NH −3.74 ppm, *meso*-H 10.18 ppm)], suggest a reduced ring current which may indicate localized conjugation pathways within the 72-atom macrocycle. Although the ring current is a major contributor to the chemical shift,[17] it is not the only factor, and effects such as conformational changes have to be taken into account. However, on the basis of the X-ray crystal structure of $(H_4{-}H_2{-}H_4)^{4+}$•**1**, at least for the tetraethylporphyrin moiety, deviation from planarity seems negligible. The *meso*-protons of the tetraethylporphyrin moiety are shifted to higher field (δ 9.30 ppm) compared with the *meso*-signal in H_2OEP; this is probably also a consequence of a reduced localized ring current.

Two reversible, spectroscopically distinct steps can be observed upon protonation of ($H_2{-}H_2{-}H_2$)•**1** with TFA in CH_2Cl_2. Protonation takes place first on the edge moieties to yield a green tetracationic species [$(H_4{-}H_2{-}H_4)^{4+}$•**1**] [visible maxima 412, 440, 489, 655, 848 nm] which was studied by X-ray crystallography (Figure 1). Upon addition of excess TFA, protonation of the central porphyrin yields the red hexaprotonated species $(H_4{-}H_4{-}H_4)^{6+}$•**1**, which exhibits split Soret bands at 432 and 511 nm and one broad Q-band at 825 nm. The X-ray structure of $(H_4{-}H_2{-}H_4)^{4+}$•**1** revealed an overall geometry somewhat different from that of $(Ni{-}H_4{-}Ni)^{2+}$•**2** (Figure 2).[12] The asymmetric unit of $(H_4{-}H_2{-}H_4)^{4+}$•**1** contained one of the terminal dicationic macrocycles and half of the central free-base macrocycle (with an inversion center in the middle of the center macrocycle). Core hydrogens in the tetraethyl macrocycle were localized on the nonfused diethylpyrrolic moieties as

(13) Seybold, P. G.; Gouterman, M. *J. Mol. Spectrosc.* **1969**, *31*, 1.
(14) Credi, A.; Prodi, L. *Spectrochim. Acta, A* **1998**, *54*, 159.
(15) Parkin, S. R.; Moezzi, B.; Hope, H. *J. Appl. Crystallogr.* **1995**, *28*, 53.
(16) Nguyen, L. T.; Senge, M. O.; Smith, K. M. *J. Org. Chem.* **1996**, *61*, 998.
(17) Sheer, H.; Katz, J. J. In *Porphyrins and Metalloporphyrins*; Smith, K. M., Ed.; Elsevier: Amsterdam, 1975; p 399.

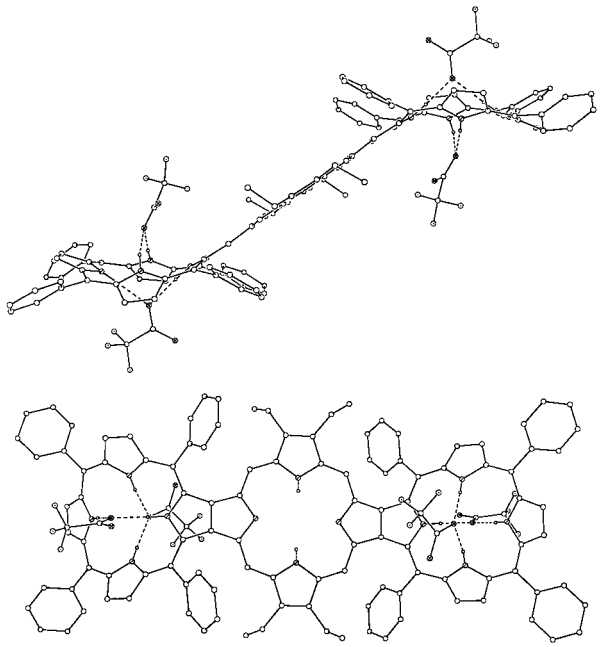

Figure 1. Molecular structure of $(H_4-H_2-H_4)^{4+}$•**1**, $4(CF_3COO^-)$: (top) side view; (bottom) top view (hydrogen atoms, except for those in the porphyrin cores, have been omitted for clarity).

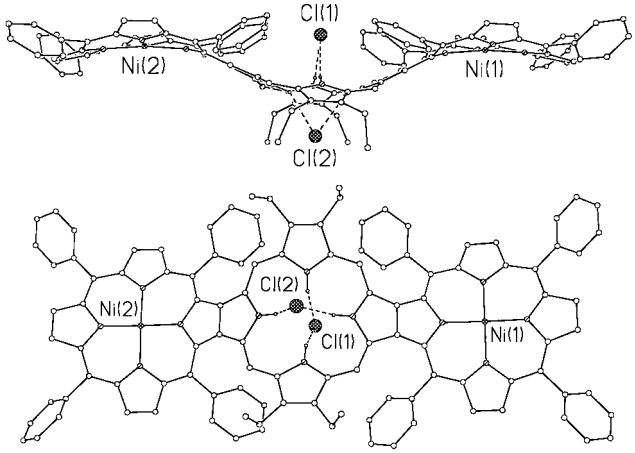

Figure 2. Molecular structure of $(Ni-H_4-Ni)^{2}$•**2**, $2(Cl^-)$: (top) side view; (bottom) top view (hydrogen atoms, except for those in the central porphyrin core, have been omitted for clarity).

shown in Figure 1. The terminal macrocycles were distorted into saddled conformations with MDPMPs[18] of 0.461 Å, whereas the central free-base macrocycle exhibited a minimally distorted waved conformation with a MDPMP of 0.035 Å. This contrasts with $(Ni-H_4-Ni)^{2+}$•**2** in which all three macrocycles exhibited saddled conformations (MDPMPs: edge macrocycles 0.419 and 0.429 Å, central macrocycle 0.376 Å). Literature precedent regarding the X-ray structures of the TPP dications $(H_4TPP)^{2+}$•$2(ClO_4^-)$[19] and $(H_4TPP)^{2+}$•(Cl^-)•$(FeCl_4^-)$[20] revealed saddled conformations with MDPMPs of 0.417 and 0.524 Å, respectively. As such, for the dicationic macrocycles of $(H_4-H_2-H_4)^{4+}$•**1**, we can attribute the saddled conformations as predominately occurring due to core congestion rather than to steric effects imposed by the fused pyrrolic moieties. However, for the tetraethylporphyrin moiety of $(Ni-H_4-Ni)^{2+}$•**2**, the saddled conformation is likely due to a combination of steric constraints from both the core and periphery of the macrocycle.

In $(H_4-H_2-H_4)^{4+}$•**1** the terminal macrocycles were coplanar with an interplanar separation of 6.48 Å[21] and formed interplanar angles of 32.4° with the central macrocycle. Again, in $(Ni-H_4-Ni)^{2+}$•**2** the terminal macrocycles were nearly coplanar (interplanar angle 2.1°) but sharply contrasted with those of $(H_4-H_2-H_4)^{4+}$•**1** in that their interplanar separation was only 0.30 Å. Of further disparity with $(H_4-H_2-H_4)^{4+}$•**1**, the central macrocycle of $[Ni-H_4-Ni]^{2+}$•**2** was nearly coplanar with the terminal macrocycles (interplanar angles 1.8° and 3.6°). In both structures, the fused pyrrole ring moieties (each comprised of an eight-atom diaza bicyclic system) were planar. Additionally, in the structure of $(H_4-H_2-H_4)^{4+}$•**1**, this planar portion of the molecule also included the tetraethyl macrocycle. The major differences between the geometries of these two structures are a result of the conformations adopted by their central porphyrin macrocycles as can be observed by comparing the side views from Figures 1 and 2. Another aspect of note regarding the structures of $(H_4-H_2-H_4)^{4+}$•**1**, $(Ni-H_4-Ni)^{2+}$•**2**, and related porphyrins bearing fused pyrrole (**5**−**7**)[10] or benzene rings (**10**),[22] lies in the $C_\beta-C_\beta$ bond lengths (Table 1). As shown, the fused $C_\beta-C_\beta$ bonds are consistently longer than the nonfused $C_\beta-C_\beta$ bonds.

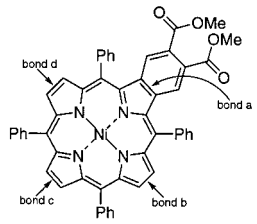

10

Optical Properties. The degree of electronic communication between macrocycles is of fundamental importance to the potential applications of porphyrin arrays. These interactions can be investigated by various methods, depending upon which property is under investigation (such as electron transfer, electronic conduction, and optical properties).[7,23,24] Optical properties are useful tools to explore the degree of π-electron delocalization; in this work we studied whether the optical transitions are localized over a single monomer or spread over the entire system. To achieve this objective, we utilized a quantum chemistry method to calculate excited states and an orbital localization technique (see, for example, refs 25 and 26).

We used a semiempirical quantum chemistry approach, INDO/SCI,[27,28] which has been parametrized to calculate absorption spectra of organic molecules. Some porphyrin oligomers have been recently studied by application of this method.[24] The simulations were performed by using the

(18) MDPMP refers to the mean deviation of the 24 macrocyclic atoms from their porphyrin mean plane; in metalloporphyrins the position of the metal is not included in this calculation.

(19) Cheng, B.; Munro, O. Q.; Marques, H. M.; Scheidt, W. R. *J. Am. Chem. Soc*. **1997**, *119*, 10732.

(20) Stone, A.; Fleischer, E. B. *J. Am. Chem. Soc*. **1968**, *90*, 2735.

(21) For the interplanar angle and interplanar separation, measurements were made as per Clement, T. E.; Nurco, D. J.; Smith, K. M. *Inorg. Chem.* **1997**, *37*, 11150.

(22) Vicente, M. G. H.; Jaquinod, L.; Khoury, R. G.; Madrona, Y.; Smith, K. M. *Tetrahedron Lett*. **1999**, *40*, 8763.

(23) Kutzler, F. W.; Ellis, D. E. *J. Chem. Phys.* **1986**, *84*, 1033.

(24) (a) Belijonne, D.; O'Keefe, G. E.; Harner, P. J.; Friend, R. H. (b) Anderson, H. L.; Bredas, J. L. *J. Chem. Phys.* **1997**, *106*, 9439.

(25) Thompson, M. A.; Zerner, M. C. *J. Phys. Chem*. **1990**, *94*, 3820.

(26) (a) Ishikawa, N.; Kaizu, Y. *Chem. Phys. Lett*. **1994**, *228*, 625. (b) Ishikawa, N.; Kaizu, Y. *J. Phys. Chem*. **1996**, *100*, 8722.

(27) Ridley, J.; Zerner, M. C. *Theor. Chim. Acta* **1973**, *32*, 111.

(28) Bacon, A.; Zerner, M. C. *Theor. Chim. Acta* **1979**, *53*, 21.

Table 1. $C_\beta-C_\beta$ Bond Lengths (Å) from the X-ray Crystal Structures of Porphyrins Bearing a Fused Aromatic Ring[a]

	compd **1**	compd **2**	compd **5**[10]	compd **6**[10]	compd **7**[10]	compd **10**[21]
bond a	**1.372(7)**	**1.37(2)**	**1.406(12)**	**1.394(8)**	**1.401(8)**	**1.395(9)**
bond b	1.351(7)	1.34(2)	1.355(11)	1.351(8)	1.340(8)	1.331(9)
bond c	1.349(8)	1.34(2)	1.318(12)	1.352(9)	1.358(8)	1.344(10)
bond d	1.347(7)	1.33(2)	1.340(12)	1.353(8)	1.353(9)	1.340(10)
bond e	**1.372(7)**	**1.382(14)**				
bond f	1.351(7)	1.33(2)				
bond g	1.349(8)	1.35(2)				
bond h	1.347(7)	1.34(2)				
bond i	1.355(8)	1.36(2)				
bond j	1.355(8)	1.369(14)				

[a] Values shown in **bold** correspond with the fused bond lengths.

MOCINDO program;[29] this program has been successfully used in a study of the optical properties of an expanded corrole.[30] When required, the molecular geometry was optimized by the commonly available PM3 method.[31]

In our orbital localization approach, we express the *i*th molecular orbital of the trimer (TMO), ψ^i, as a linear combination over all monomer molecular orbitals (MMOs) ϕ_{nj}:

$$|\psi^i\rangle = \sum_n \sum_j d^i_{nj} |\phi_{nj}\rangle \qquad (1)$$

where $n = 1$, 2, and 3 is the index for the monomer.

The considered MMOs are the molecular orbitals of the isolated porphyrins, and thus they are completely localized over the respective monomer. Compared to other approaches,[25,26] we do not discriminate in eq 1 between occupied or unoccupied orbitals: this gives us a more general expansion. In the case of a β-fused trimer, the determination of the coefficients d^i_{nj} requires a solution of an underdetermined system because the number of the TMOs will be less than 3 times the number of MMOs; in this case the minimum norm solution has been chosen.

Using this localization technique, the *k*th excited states of the trimer, Ψ^k, (calculated using configuration interaction with single excitations over π-orbitals) was expressed in terms of *excitonic* transition (excitation over a single monomer) or *charge-transfer* transition (electronic transfer between different monomers):[25,26]

$$|\Psi^k\rangle = \sum_{nj} \sum_{n'j'} c^k_{nj \rightarrow n'j'} |\phi_{nj} \rightarrow \phi_{n'j'}\rangle \qquad (2)$$

Summing over all MMOs, it is possible to associate, with each excited state, a 3×3 matrix (called the M-matrix):

$$m^k_{nn'} = \sum_{jj'} |c^k_{nj \rightarrow n'j'}|^2$$

An excited state with a diagonal M-matrix is thus characteristic of a system with only excitonic resonance between monomers, whereas the off-diagonal terms are a measure of the excitation delocalization over the complete trimer. This method can be generalized for longer oligomers and offer a systematic analysis of the electron−hole wave function[32] in terms of electronic transition between monomers.

(29) Della Sala, F.; Di Carlo, A.; Lugli, P. In-house developed INDO/S code based on QCPE No. 372.

(30) Paolesse, R.; Khoury, R. G.; Della Sala, F.; Di Natale, C.; Sagone, F.; Smith, K. M. *Angew. Chem., Int. Ed. Engl.* **1999**, *38*, 2577.

(31) Stewart, J. J. P. *J. Comput. Chem.* **1989**, *10*, 209.

(32) Köhler, A.; dos Santos, D. A.; Belijonne, D.; Shuai, Z.; Bredas, J. L.; Holmes, A. B.; Kraus, A.; Müllen, K.; Friend, R. H. *Nature* **1998**, *392*, 903.

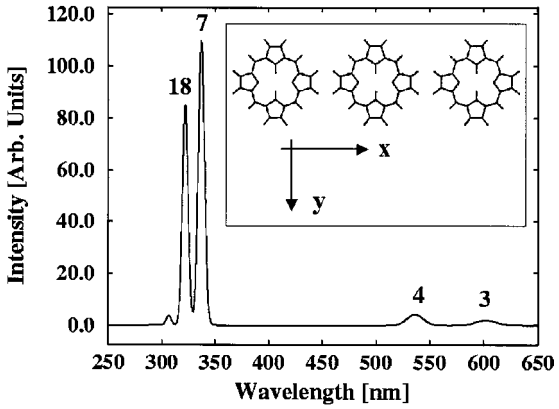

Figure 3. INDO/SCI absorption spectra of three separated porphyrins. The inset shows the structure with the axis indication.

As a quantitative variable we define α^k, the *degree of excitonic contribution* for the *k*th excited state:

$$\alpha^k = \mathrm{Tr}[\mathrm{M}^k] = \sum_n m^k_{nn}$$

As a starting point of the analysis we consider three *separated* porphyrins, and we treat them as a supermolecule;[25] the center-to-center distance between macrocycles has been fixed at 12 Å (along the *x*-axis), as shown in the inset in Figure 3. In this case, the interactions between monomers are expected to be only excitonic, and thus $\alpha = 1$ for all the optically active excited states; other charge resonance states[25] are optically forbidden. When the interactions between monomers are only excitonic, the excited-state wave function of the trimer can be expressed as

$$|\Psi^k\rangle = |\Psi^{h,i}\rangle = \sum_n e^i_n |\Phi^h_n\rangle \qquad (3)$$

where Φ^h_n is the *h*th excited state of monomer *n*. Each excited state of the trimer can be expressed as a linear combination of the same monomer excited state; referring to eq 3, the monomer excited state Φ^h will be called the *excitonic origin* of the trimer excited state Ψ^k (which can be labeled as $\Psi^{h,i}$, where *i* is an integer).

We note also that the elements of the M-matrix are

$$m^{h,i}_{nn'} = \delta_{nn'} |e^i_n|^2 \qquad (4)$$

The INDO/SCI energies, oscillator strengths, polarizations, M-matrix elements, and excitonic origins are reported in Table 2. The calculated absorption spectrum is reported in Figure 3; an arbitrary Gaussian broadening has been used, and no vibronic

Table 2. Excited-State Analysis for Three Separated Porphyrins[a]

no.	λ (nm)	f_{osc}	pol	$1 \rightarrow 1$ (%)	$2 \rightarrow 2$ (%)	$3 \rightarrow 3$ (%)	exc orig
1	603.4	0.0017	Y	21.4	57.2	21.4	Q_y
2	602.8	0.0000		50.0	0.0	50.0	Q_y
3	602.0	0.1525	Y	28.6	42.8	28.6	Q_y
4	536.5	0.3354	X	25.9	48.2	25.9	Q_x
5	531.9	0.0000		50.0	0.0	50.0	Q_x
6	528.7	0.0039	X	24.1	51.8	24.1	Q_x
7	337.0	8.5755	X	25.9	48.0	25.9	B_x
8	335.3	0.1602	Y	23.5	52.9	23.5	B_y
13	329.2	0.0000		49.7	0.1	49.7	B_y
18	321.9	6.7935	Y	26.5	47.0	26.5	B_y
19	318.8	0.0000		47.7	4.5	47.7	B_x
20	306.7	0.2803	X	29.4	41.3	29.4	B_x

[a] For each excitonic excited state are reported its number (no.), the wavelength (λ) of excitation, the oscillator strength (fosc), the polarization (pol), the percentage of excitonic contribution on each monomer (**1** → **1**, **2** → **2**, **3** → **3**), and the excitonic origin (exc orig) (see the text).

replicas have been included. It must be noted that the INDO/SCI technique is known to overestimate the energy of the Soret band.[33,34]

Excitonic interactions between monomers create a splitting in the B (Soret) and Q (visible) bands that can also be analyzed considering a simple dipole−dipole interaction model.[35]

The term $m_{nn}^{h,i}$ specifies the percentage of excitation over the monomer n; from eq 4 we see that this is directly related to the coefficient e_n^i, approximately the eigenvectors of the excitonic Hamiltonian:

$$H = \begin{bmatrix} \Delta E & \gamma & 0 \\ \gamma & \Delta E & \gamma \\ 0 & \gamma & \Delta E \end{bmatrix}$$

where γ is the excitonic resonance interaction between first neighbor monomers and ΔE is the single monomer transition energy.

We note also that the transitions with nonzero oscillator strength are mainly localized over the central monomer. The closer the porphyrins, the greater the splitting of Q- and B-bands. It is not possible to consider the porphyrins at a center-to-center distance of less than 12 Å that would lead to atom superimposition; for this reason we consider a β-fused trimer in a fully planar configuration. This system (see the inset in Figure 4) has been analyzed with the previous described method. The absorption spectrum calculated with the INDO/SCI approach is shown in Figure 4. Compared to the three separated porphyrins, significant overlap of monomer orbitals occurs, and thus the simple analysis adopted in the previous case will not hold.

The results of the localization procedure (Table 3) can be used to investigate the nature of excited states. Analysis of this table shows that the main peaks (1, 2, 4, 6, 8) are not completely of excitonic origin. However, the excitonic contribution is prevalent (α > 60%), and as expected from the separated porphyrin case, the excitation is predominant on the central part. The polarization of the strongest transitions (1, 8) is along the long axis of the molecule (x-axis). The excitonic origin reported in Table 3 is, in this case, only due to mixing of the excited state; however, all the first six excited states come from the Q-bands.

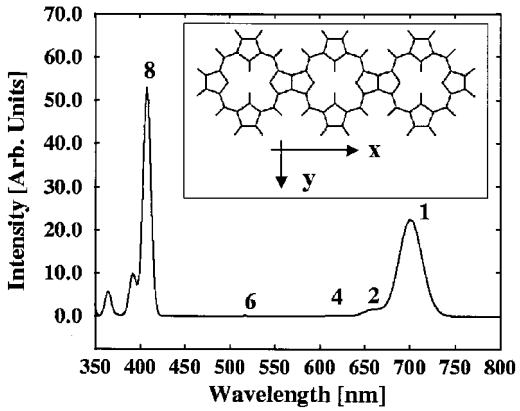

Figure 4. INDO/SCI absorption spectra of an ideal planar trimer. The inset shows the structure with the axis indication.

The complete electron−hole wave function[31] for the first excited state is reported in Figure 5. Here we do not consider the hole localized on an atom,[31] but on a monomer. Thus, this plot has been obtained considering as the weight (P_β) on each atomic wave function (β) the following expression:

$$P_\beta = \sum_\alpha |c_{\alpha\rightarrow\beta}|^2 W_\alpha$$

where $c_{\alpha\rightarrow\beta}$ is the CI-coefficient for the trimer considering the atomic wave function as basis set and α (the hole) moves over on all atomic wave functions of the central monomer. As a weighting coefficient we use

$$W_\alpha = [\sum_\gamma |c'_{\alpha\rightarrow\gamma}|^2]^{1/2}$$

where $c'_{\alpha\rightarrow\gamma}$ is the CI-coefficient for the central monomer considering the atomic wave function as the basis set: this weighting coefficient accounts for the single monomer excitonic wave function.

Thus, P_β represents the probability of finding an electron on atomic wave function β, considering that the hole is confined in the central porphyrin; from Figure 5 we see that the probability of finding the electron is much greater in the central ring, as expected from the high value of α.

We conclude that even if the optical transitions cannot be described within the exciton model, the π-electron system *is not completely extended over the 72-atom macrocycle*. We can argue that the stability of each monomer ring system is strong enough to prevent the complete delocalization over the system; thus, even for higher oligomers and polymers, the exciton wave function will be completely localized over three porphyrin units.

We have assumed a planar conformation for this β-fused trimer; X-ray characterization of $(H_4-H_2-H_4)^{4+}$·**1** shows, however, a nonplanar conformation of the molecule. Also if it is reasonable to attribute molecular distortions in $(H_4-H_2-H_4)^{4+}$·**1** to the core protonation of the terminal porphyrin subunits, we have no information on the effective conformation of $(H_2-H_2-H_2)$·**1**. Geometry optimization starting from the X-ray data did not afford significant results, and due to the complexity of the system and to the high number of degrees of freedom, the real geometry of $(H_2-H_2-H_2)$·**1** is difficult to determine accurately.

To study the influence of the molecular geometry on the optical properties of these molecules, we decided to assume for $(H_2-H_2-H_2)$·**1** the nonplanar molecular geometry observed in the X-ray data obtained from $(H_4-H_2-H_4)^{4+}$·**1**. To calculate

(33) Rawlings, D. C.; Davidson, E. R.; Gouterman, M. *Theor. Chim. Acta* **1982**, *61*, 227.
(34) Baker, J. D.; Zerner, M. C. *Chem. Phys. Lett.* **1990**, *175*, 192.
(35) Pope, M.; Swenberg, C. E. In *Electronic Process in Organic Crystal*; Clarendon Press: Oxford, UK, 1962.

Table 3. Excited-State Analysis for the Planar Trimer[a]

no.	λ (nm)	f_{osc}	pol	1 → 1, 3 → 3 (%)	1 → 2, 3 → 2 (%)	1 → 3, 3 → 1 (%)	2 → 1, 2 → 3 (%)	2 → 2 (%)	α (%)	exc orig
1	700.6	1.7870	X	12.9	9.8	1.1	6.8	38.6	64.4	Q_x
2	660.4	0.1306	Y	14.4	5.1	0.2	3.6	53.4	82.2	Q_y
3	633.9	0.0000		42.7	3.7	0.3	3.2	0.3	85.7	Q_y
4	618.6	0.0192	Y	28.6	3.6	0.1	2.4	30.6	87.8	Q_y
5	567.4	0.0000		37.6	7.8	0.2	3.2	2.4	77.7	Q_x
6	516.8	0.0089	X	27.2	2.4	0.1	2.3	36.0	90.4	Q_x
7	437.9	0.0000		1.8	15.8	7.7	17.6	14.4	17.9	
8	407.8	3.8573	X	15.4	12.1	2.4	2.1	35.9	66.7	B_x, Q_x
9	404.5	0.3853	Y	3.6	11.0	1.2	13.3	41.6	48.8	B_y, Q_y
10	402.6	0.0000		8.2	6.3	4.1	24.9	13.0	29.4	
11	394.8	0.1198	Y	7.0	11.5	3.6	22.8	10.2	24.2	

[a] For each excitonic excited state are reported its number (no.), the wavelength (λ) of excitation, the oscillator strength (f_{osc}), the polarization (pol), the element of the M-matrix in percentage (some of these are equal for symmetry consideration), the degree of excitonic contribution (α), and the excitonic origin (exc orig) specified only for states with (α > 30) (see the text for further details).

Table 4. Excited-State Analysis for the Real Trimer[a]

no.	λ (nm)	f_{osc}	pol	1 → 1, 3 → 3 (%)	1 → 2, 3 → 2 (%)	1 → 3, 3 → 1 (%)	2 → 1, 2 → 3 (%)	2 → 2 (%)	α (%)
1	744.3	1.5963	X	16.6	9.2	1.3	7.6	30.3	63.6
2	689.1	0.1008	XY	32.0	4.6	0.4	4.0	14.8	81.5
3	684.0	0.0000		43.1	4.6	0.4	3.3	0.2	83.9
4	637.5	0.0326	Y	7.6	5.1	0.1	2.9	68.7	83.7
5	603.8	0.0000		39.0	5.1	0.2	4.4	2.6	80.6
6	535.3	0.2114	XY	29.3	1.9	0.1	2.8	31.9	90.4
7	454.4	0.0000		2.6	11.3	7.7	20.6	15.1	20.4
8	420.9	0.0029	XY	11.5	8.3	4.5	26.6	3.8	25.4
9	419.6	1.8164	XY	11.0	6.7	4.6	15.0	19.9	43.4
10	414.7	2.9807	XY	14.2	5.4	2.6	12.0	31.2	59.8

[a] For each excitonic excited state are reported its number (no.), the wavelength (λ) of excitation, the oscillator strength (f_{osc}), the polarization (pol), the element of the M-matrix (some of these are equal for symmetry consideration) in percentage, and the degree of excitonic contribution (α).

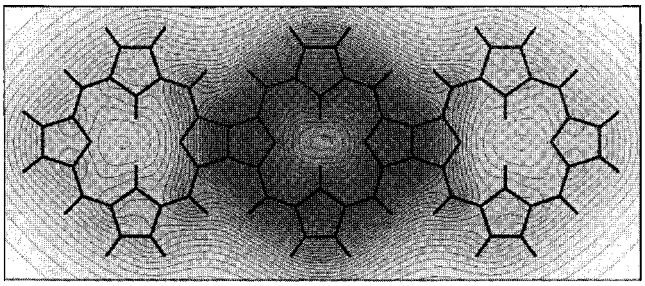

Figure 5. Electron−hole wave function for the first state of the ideal planar trimer. Contour curves are the zones of equal probability of finding an electron considering the hole localized on the central monomer (see the text for details); the probability will be higher in the darker zones.

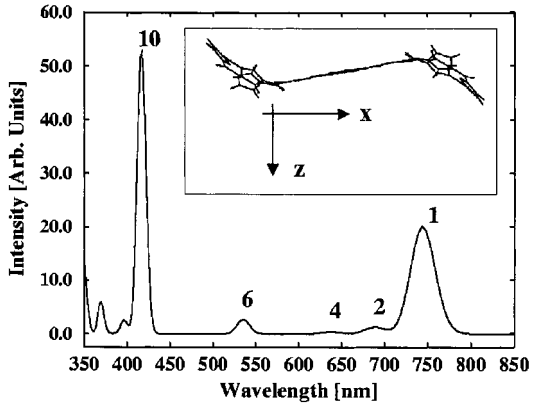

Figure 6. INDO/SCI absorption spectra of a real trimer. The inset shows the X-ray structure with the axis indication.

the optical properties of this structure, peripheral substituents were removed to have a direct comparison with the previous planar case, and because the substituents have little effect (red shift) on the optical properties. The INDO/SCI absorption spectrum for the considered molecular geometry is reported in Figure 6.

The main transitions of the planar and the nonplanar trimers are similar; distortion does not destroy the exciton delocalization. We note also that the calculated transition energies and oscillator strengths are sensitive to molecular geometry changes, but the localization properties are invariant. In Table 4 the results of the localization for the nonplanar trimer are reported. The coefficient of the M-matrix is comparable with those in Table 3. Using the X-ray data, we found good agreement with the experimental absorption spectrum (Figure 7).

We note also that due to the low symmetry of the X-ray geometry (C_i), the polarization is slightly different from that of the previous ideal case; also due to the high molecular distortion, it is not possible to extract any significant excitonic origin.

Photophysical Properties of the Fused Triad. The experimental absorption spectrum of $(H_2-H_2-H_2)$·**1** in CH_2Cl_2 is shown in Figure 7. As can be seen, the Soret bands and Q-bands are markedly shifted toward longer wavelength with respect to the reference compound (H_2TPP), indicating a good degree of π-electron delocalization in the trimer. This is confirmed by the theoretical values α, and by the evidence that the optical transition cannot be completely described with the excitonic (i.e., localized over the single monomers) model. A similar spectrum was also recorded in methylcyclohexane. In these solvents, $(H_2-H_2-H_2)$·**1** shows good chemical stability even if irradiated with UV or visible light.

At room temperature in CH_2Cl_2 and methylcyclohexane solutions, and at 77 K in a transparent rigid methylcyclohexane

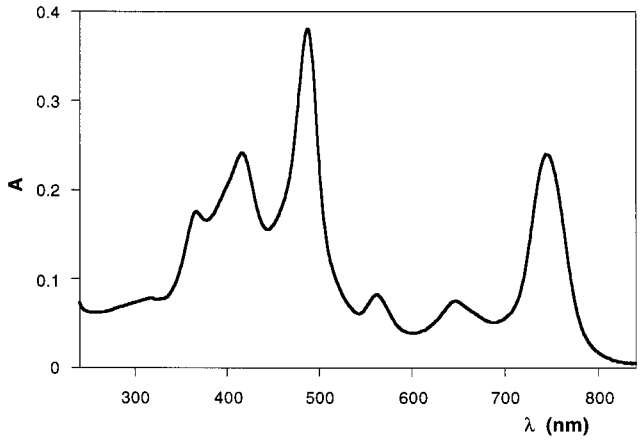

Figure 7. Absorption spectrum of $(H_2-H_2-H_2)$•**1** in CH_2Cl_2 at room temperature.

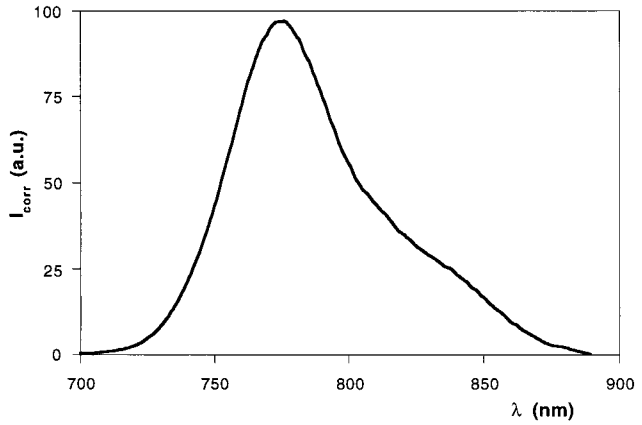

Figure 8. Fluorescence spectrum of $(H_2-H_2-H_2)$•**1** in CH_2Cl_2 at room temperature.

matrix, trimer $(H_2-H_2-H_2)$•**1** displays a very intense fluorescence band ($\Phi = 0.09$ and $\tau = 2.0$ ns at room temperature), with a maximum at 775 nm (Figure 8). The excitation spectrum strictly matches the absorption analogue, indicating that excitation over all the 240−780 nm region leads to the population of the fluorescent excited state with unitary efficiency. The very low Stokes shift observed suggests that the distortion occurring on going from the ground state to the excited state is also very low. This indicates that for the fluorescent excited state the contribution coming from transitions in which a large charge separation is achieved (as in the case of electronic transfer between different monomers) is almost negligible, again in agreement with the conclusions from the theoretical study. All this discussion can lead, also by analogy with the monomeric porphyrin, to the attribution of this band to the singlet of the lowest $\pi^* \rightarrow \pi$ transition of the extended π-system. Such an intense band is quite rare in the 750−900 nm range. For this reason, $(H_2-H_2-H_2)$•**1** could be a good candidate for labels and sensors working in biological media where luminescence in this spectral region is of particular interest, and a good reference for measuring quantum yields in the near-infrared. No phosphorescence was observed, and we believe it to lie in a region outside the instrumental range (900 nm being the upper limit).

Conclusions

A synthetic methodology has been developed for the preparation of oligomeric porphyrin arrays in which the porphyrinic macrocycles are directly fused through their β-pyrrolic carbons. Via this technique we demonstrate the preparation of fused linear porphyrin trimers **1** and **2** which feature 62-π-electron 72-atom aromatic macrocycles. Crystallographic characterization of **1** (as its tetracation salt) and **2** (as its dication salt) revealed that this type of molecule bears a considerable degree of macrocyclic flexibility. Future work utilizing this framework bears the potential to make use of a variety of methods (i.e., core and peripheral substitution, metalation, axial ligation) to achieve specific overall molecular conformations. The emission spectrum of $(H_2-H_2-H_2)$•**1** demonstrated a fluorescence band at 775 nm, indicating significant interactions between the porphyrin moieties in the trimer. To obtain further information on the possible applications of $(H_2-H_2-H_2)$•**1**, we studied the degree of π-electron delocalization, using a semiempirical quantum chemistry approach and localization technique. To have indications of the importance of the molecular conformations on the electronic properties of this oligoporphyrin, our study was carried out both assuming the geometry obtained from the X-ray characterization and on an ideal planar β-fused porphyrin trimer. These studies showed that the optical properties of **1** cannot be described within the excitonic model of weakly interacting macrocycles ($\alpha > 60\%$), but that π-electron delocalization over the 72-atom macrocycle is not complete. Even though resonance structures for the 72-atom macrocycle imply a fully conjugated aromatic system, our data indicated that the three constituent porphyrin macrocycles behave somewhat more like discrete aromatic systems. Finally, thanks to its high-intensity luminescence in the near-IR region, compounds such as $(H_2-H_2-H_2)$•**1** might be used as a chromophore for labels and sensors working in biological media.

Acknowledgment. Support from CNR-MADESS II (Italy) and from the National Science Foundation (Grant CHE 99-04076) is gratefully acknowledged.

Supporting Information Available: Tables of crystallographic data (PDF, CIF). This material is available free of charge via the Internet at http://pubs.acs.org.

JA001316+